Raman Heterodyne Detection of Radio-Frequency Resonances in Sm Vapor: Effects of Velocity-Changing Collisions

J. Mlynek, Chr. Tamm, E. Buhr, and N. C. Wong[a]
Institut für Quantenoptik, Universität Hannover, 3000 Hannover 1, Federal Republic of Germany
(Received 31 July 1984)

Raman heterodyne detection of rf-generated sublevel coherence is investigated in atomic samarium vapor under conditions of velocity-selective optical pumping. In the presence of rare-gas perturbers, velocity-changing collisions determine the characteristics of the rf-laser double-resonance signals by strongly affecting their linewidths and line shapes. The results can be quantitatively explained by a theoretical model that includes velocity-diffusion processes.

PACS numbers: 42.65.Cq, 32.80.−t, 34.90.+q, 35.80.+s

Recently, a novel rf-laser double-resonance method for optical heterodyne detection of sublevel coherence phenomena was introduced.[1] This so-called Raman heterodyne technique relies on a coherent Raman process being stimulated by a resonant rf field and a laser field [see Fig. 1(b)]. So far, the method has only been applied to impurity-ion solids for studying nuclear magnetic resonances at low temperature.[1-3] It is the aim of this communication to investigate Raman heterodyne detection of rf-induced sublevel coherence in the gaseous phase. Here, in fact, the Raman heterodyne technique extends previous methods in optical-pumping double resonance using incoherent light sources.[4] In the case of Doppler-broadened optical transitions, however, new signal features are expected to appear as a result of velocity-selective optical pumping (VSOP) caused by the narrow-bandwidth laser excitation. As a specific example, we report studies on Zeeman resonances in a $J=1 \rightarrow J'=0$ transition in atomic samarium vapor.[5]

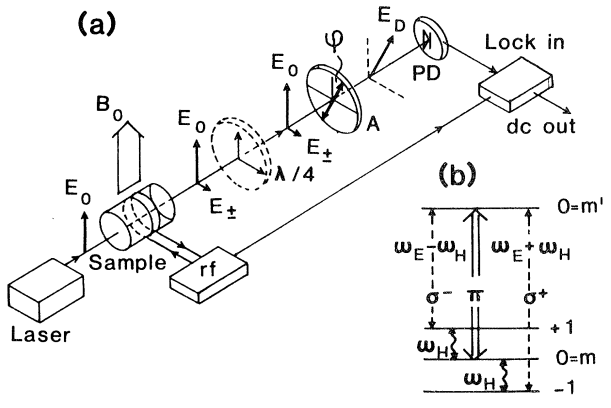

FIG. 1. (a) Experimental scheme. The $\lambda/4$ plate is used for detection of the FM-Raman heterodyne signal (see text). A, polarization analyzer; PD, photodetector; B_0, static magnetic field. (b) Energy level diagram for a Zeeman split $J=1 \rightarrow J'=0$ transition, showing the coherent Raman process.

The basic coherent Raman process for a Zeeman split $J=1 \rightarrow J'=0$ transition is shown in Fig. 1(b); the schematic of our experimental arrangement for Raman heterodyne detection is shown in Fig. 1(a). The laser field $\vec{E}_0$ of frequency ω_E is polarized parallel to a transverse static magnetic field $\vec{B}_0$ that lifts the ground-state Zeeman-level degeneracy. The field $\vec{E}_0$ only drives the optical π transition ($m-m'=0$) and thereby optically pumps the ground-state Zeeman sublevels. In the limit of slow ground-state relaxation, it efficiently produces an alignment in the ground-state m sublevels. A longitudinal rf field of frequency ω_H can now resonantly excite $|\Delta m|=1$ coherences and, via a two-photon process, the simultaneous presence of the light field $\vec{E}_0$, gives rise to coherent Raman sidebands $\vec{E}_\pm$ with frequencies $\omega_E \pm \omega_H$. As a consequence of the selection rules the Stokes ($\vec{E}_-$) and anti-Stokes ($\vec{E}_+$) fields are σ^- and σ^+ polarized, respectively, i.e., their direction of polarization is perpendicular to the driving light field $\vec{E}_0$. Behind the sample the total light field consists of orthogonally polarized carrier ($\vec{E}_0$) and Raman sideband ($\vec{E}_\pm$) components with modulation frequency ω_H. The optional retardation plate behind the sample cell is oriented with its axes parallel to these polarization directions; it thus only introduces a constant phase shift θ between the carrier and the Raman sidebands with $\theta=\pi/2$ for a $\lambda/4$ plate. A polarization analyzer that is inserted under an angle ϕ with respect to the z axis is then used to project the carrier and the Raman sidebands along a common direction [see Fig. 1(a)]. At the photodiode the strong optical carrier finally serves as a local oscillator for heterodyne detection of the Raman sidebands.

To predict the characteristics of the coherent Raman signal for a $J=1 \rightarrow J'=0$ transition we have

performed a steady-state density-matrix calculation for an inhomogeneously broadened four-level system taking into account VSOP. Details of this treatment will be given elsewhere[6]; here we will only discuss the main results. With m_{AM} and m_{FM} denoting the modulation depth of the amplitude and frequency modulation of the resulting field $\vec{E}_D(t)$ due to the Raman sidebands,[2] the heterodyne beat signal at the detector is of the form

$$|E_D|^2_{\mathrm{beat}} = 2E_0 \sin\phi \cos\phi [E_0 \cos\theta \{\mathrm{Re}(m_{\mathrm{AM}})\cos\omega_H t + \mathrm{Im}(m_{\mathrm{AM}})\sin\omega_H t\} - E_0 \sin\theta \{\mathrm{Re}(m_{\mathrm{FM}})\cos\omega_H t + \mathrm{Im}(m_{\mathrm{FM}})\sin\omega_H t\}]. \quad (1)$$

If we neglect the effect of collisions, the generalized modulation depths m_{AM} and m_{FM} containing phase-sensitive information on the rf resonance are given by simple expressions that clearly reveal the different origins of the AM- and FM-Raman signals:

$$m_{\mathrm{AM}} = K \frac{\gamma_g - i\Delta_H}{\Delta_H^2 + \gamma_g^2} \exp\left[-\left(\frac{\Delta_E}{\sigma_E}\right)^2\right], \quad (2)$$

$$m_{\mathrm{FM}} = K \frac{\gamma_g - i\Delta_H}{\Delta_H^2 + \gamma_g^2} \exp\left[-\left(\frac{\Delta_E}{\sigma_E}\right)^2\right] \frac{2\Gamma}{\sigma_E} \frac{\Delta_E}{\sigma_E}, \quad (3)$$

$$K = \frac{NL\pi^{1/2}\omega_E^2 \mu_0}{9\hbar^2 k \sigma_E} \frac{\mu_{24}^2 E_0^2}{\gamma_g \Gamma \hbar^2} \mu_{12}\mu_{24}\mu_{41} H. \quad (4)$$

Here $\vec{k}$ is the optical propagation vector, N the atomic-number density, and L the interaction length. $\Delta_E = \omega_E - \omega_{42}$ denotes the optical detuning and $\Delta_H = \omega_H - \omega_{32}$ is the rf detuning. The optical linewidth is given by Γ and the transit-time broadening of the rf linewidth is approximated by a sublevel-decay rate constant γ_g. σ_E describes the Doppler-broadened Gaussian linewidth for the optical transition. μ_{ij} is the absolute value of the transition matrix element ($\mu_{12} = \mu_{23}$, $\mu_{14} = \mu_{34}$). Equations (2)–(4) show that for the $J = 1 \rightarrow J' = 0$ transition discussed here, the AM- and FM-Raman signals are due to velocity-selective optical absorption and dispersion, respectively. Under fully resonant conditions ($\Delta_H = \Delta_E = 0$), we find $m_{\mathrm{AM}} = K/\gamma_g$ and $m_{\mathrm{FM}} = 0$; close to optical resonance ($\Delta_E \simeq \sigma_E$), Eqs. (2)–(4) yield $|m_{\mathrm{AM}}/m_{\mathrm{FM}}| = \sigma_E/2\Gamma$, i.e., the AM-Raman amplitude is generally very large compared to the FM amplitude. This stems from the fact that the laser field is always on resonance with respect to the rf-driven atoms because of VSOP; under these conditions, the presence of an FM-Raman signal is only due to the slight asymmetry of the optically pumped velocity packet within the Doppler distribution. Consequently, the FM-Raman signal should be very sensitive to velocity-diffusion processes in the sample as will also become obvious later on. The AM- and FM-Raman heterodyne signals (RHS) can be easily isolated by means of the retardation plate [see Fig. 1(a)] that introduces a phase shift θ between the carrier and the sidebands. For $\theta = 0$ (no retardation plate), the FM-RHS cancels out as expected [see Eq. (1)]; for $\theta = \pi/2$ ($\lambda/4$ plate), the FM-RHS can be monitored and the AM-RHS vanishes.

Experiments were performed on the Sm I line $\lambda = 570.6$ nm ($4f^6 6s^2\, {}^7F_1 \rightarrow 4f^6 6s 6p\, {}^7F_0$) with use of the arrangement schematically shown in Fig. 1(a). The samarium vapor was contained in a heated ceramic tube of 1 cm diam; the temperature of the vapor cell was $\simeq 1000$ K with the length of the heated zone being 3 cm. In most experiments a buffer gas (e.g., Ar) was added at a low pressure. Natural Sm consists of a mixture of seven isotopes with mass numbers 144, 147, 148, 149, 150, 152, and 154. The total Sm number density was estimated to be $\simeq 10^{13}$ cm^{-3}; the Doppler broadening $\sigma_E/2\pi$ of the optical lines is about 0.7 GHz. For optical excitation, a free-running single-mode dye ring laser with an unfocused beam diameter of 500 μm was used; its beam power was kept in the range of 0.5 to 1 mW. The rf field was produced by a simple coil surrounding the vapor cell. The polarization analyzer was set at $\phi = 45°$ and a *p-i-n* diode served for optical detection; the cosine (in-phase) component of the ac detector signal [see Eq. (1)] was demodulated in a high-frequency lock-in amplifier and then sent to a minicomputer for signal averaging.

Raman heterodyne signals of the Zeeman resonances were observed at a fixed radio-frequency $\omega_H = 2\pi \times 20.45$ MHz by varying the Zeeman splitting via the external magnetic field B_0; in these experiments the laser was tuned close to the optical resonance of the ^{154}Sm isotope ($\Delta_E = -2\pi \times 0.7$ GHz). In Fig. 2(a) typical in-phase AM- and FM-RHS are shown for the case that *no* buffer gas was added. The FM-RHS was monitored with the use of the $\lambda/4$ plate as discussed above; corresponding to the high accuracy in path length difference of the $\lambda/4$ plate used, less than 0.3% of the AM signal is present during FM detection. The different polarity of the FM-RHS is due to the chosen laser detuning

$\Delta_E < 0$ [see Eq. (3)]. According to the Landé factor of $g_J = 1.5$, the transit-time broadening of the resonances corresponds to 140 kHz (half width at half maximum) in frequency; as predicted by Eqs. (2) and (3), the linewidths are equal for AM- and FM-RHS. Moreover, the measured amplitude ratio $|m_{AM}/m_{FM}|$ of $\simeq 60$ is also in satisfactory agreement with the expected value $\sigma_E/2\Gamma = (700\ \text{MHz})/(2\times 5\ \text{MHz}) = 70$ for $|\Delta_E| = \sigma$; here $\Gamma/2\pi$ is determined by the laser linewidth of $\simeq 5$ MHz (half width at half maximum).[17] The RHS changes drastically, however, if small amounts of buffer gas are added as can be seen in Fig. 2(b): with respect to Fig. 2(a) these curves were monitored at an argon pressure of 0.65 mbar under otherwise unchanged experimental conditions. Surprisingly not only the amplitude ratio $|m_{AM}/m_{FM}|$ has become smaller, but the two curves also differ in line shape and linewidth. Similar differences in the AM- and FM-RHS were observed in the presence of helium, neon, and xenon buffer gas: Two examples are given in Fig. 3, which displays the measured linewidths of the AM- and FM-RHS for (a) xenon and (b) helium in the pressure range up to 4 mbar.

The observed differences in AM- and FM-RHS that obviously are related to collisions between Sm and buffer-gas atoms cannot be explained by Eqs. (2)–(4): The corresponding simple theory not only neglects collisional Zeeman-coherence decay but also the possibility of a collisional redistribution of atomic velocities. Although velocity-changing collisions (VCC) are known to strongly affect *optical* line shapes, it is generally assumed that *rf*-optical double-resonance line shapes are not very sensitive to VCC. If collisional Zeeman-coherence decay *and* velocity diffusion are included in our density-matrix treatment by use of an appropriate formalism,[8] the calculations clearly show that thermalizing VCC between Sm and buffer-gas atoms do play an important role in the formation of the RHS. First results of this more elaborate theory[6] with use of a Keilson-Storer collision kernel[8] for VCC are displayed as full curves in Fig. 3. In particular, our theory predicts that the linewidth of the AM-RHS is strongly influenced by VCC and that it is always larger than the width of the FM-RHS; keeping in mind that the AM-RHS originates from the optically resonant velocity subgroup, its linewidth can be interpreted as being transit-time broadened in velocity space as a result of velocity diffusion. Interestingly, if there is a sufficiently large number of VCC during the sublevel coherence lifetime, the velocity diffusion directed back into the resonant velocity subgroup becomes important and reduces the AM-RHS broadening. This effect is most obvi-

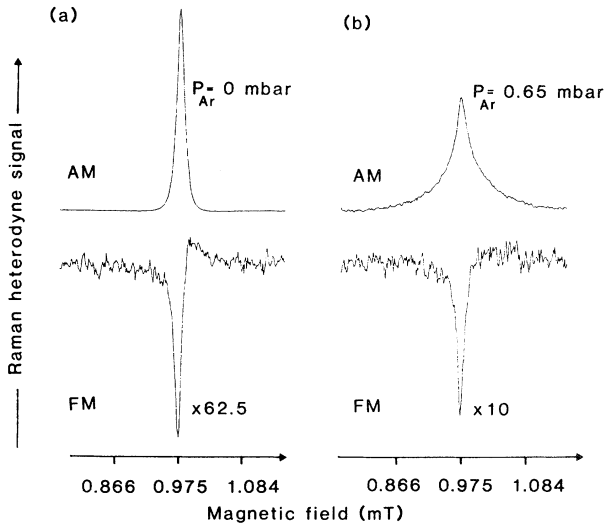

FIG. 2. In-phase Raman heterodyne signals as a function of Zeeman splitting demonstrating the different influence of foreign gas perturbers on the AM- and FM-signal amplitudes and line shapes. (a) Without buffer gas; (b) argon buffer-gas, pressure 0.65 mbar. Note the magnified scales of the FM signals.

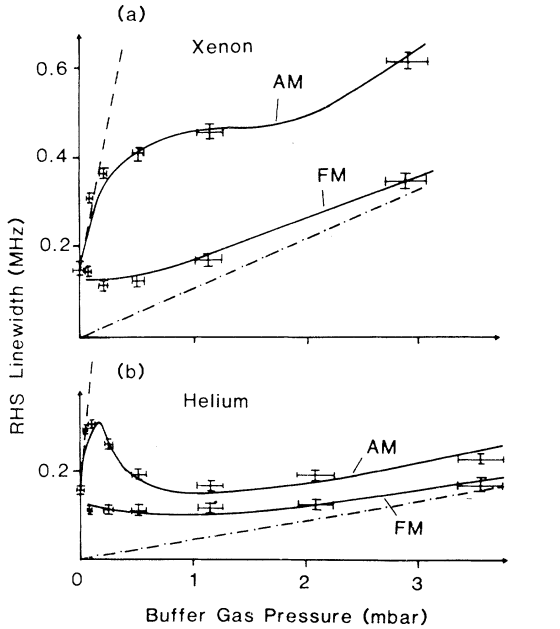

FIG. 3. Variation of the rf linewidth (half width at half maximum) of the AM- and FM-Raman heterodyne signals with buffer-gas pressure for (a) xenon and (b) helium. Experimental points are given by crosses; the full curves correspond to fits that are based on a theory including velocity-changing collisions. Dashed lines, initial slopes for AM-RHS giving γ_{VCC}; dash-dotted lines, asymptotic slopes for FM-RHS giving γ_{col}.

ous in the case of He where it gives rise to a decrease in the AM-RHS linewidth in the pressure range of 0.2–0.8 mbar. At higher perturber densities, the pressure broadening of both AM- and FM-RHS is mainly due to coherence-destroying collisions. The calculations also show that in the presence of VCC an enhanced number of atoms can yield dispersive signal contributions to the coherent Raman process: As a consequence the FM-RHS can become comparable in amplitude with the AM-RHS, which is in agreement with our observations [see Fig. 3(b)].

From the data displayed in Fig. 3 we can derive a rate constant γ_{VCC} for VCC and a rate constant γ_{col} for collisions destroying the Zeeman coherence: Theory predicts that the asymptotic slope of the FM-RHS yields γ_{col} whereas the initial slope of the AM-RHS gives γ_{VCC}. From the fitted curves in Fig. 3, the following rate constants are obtained: $\gamma_{VCC}(Xe) = 2\pi \times 1.3$ MHz/mbar, $\gamma_{col}(Xe) = 2\pi \times 110$ kHz/mbar, $\gamma_{VCC}(He) = 2\pi \times 3.0$ MHz/mbar, and $\gamma_{col}(He) = 2\pi \times 45$ kHz/mbar. Here the error in γ_{col} is $\pm 10\%$ whereas the values given for γ_{VCC} are only first estimates as a result of limited number of data points at low buffer-gas pressure. The change from heavy (Xe) to light (He) rare-gas perturbers obviously yields opposite trends for γ_{VCC} and γ_{col}; this behavior is not surprising considering the larger average thermal velocity and smaller atomic polarizability of He with respect to Xe.

In conclusion, we have reported on AM- and FM-Raman heterodyne detection of radio-frequency induced sublevel coherence in atomic Sm vapor under conditions of velocity-selective optical pumping. The comparison of AM- and FM-Raman heterodyne signals has revealed that, in the presence of rare-gas perturbers, velocity-changing collisions strongly influence the linewidth and line shape of the observed rf resonances. This work thus demonstrates that velocity diffusion can play an important role in Doppler-free double-resonance experiments involving sublevel coherence.

We are indebted to Professor Lange for stimulating discussions. One of us (Chr.T.) acknowledges support by a fellowship of the Studienstiftung des Deutschen Volkes and another (N.C.W.) by the Hannoversche Hochschulgemeinschaft. We also thank the Deutsche Forschungsgemeinschaft for financial support.

---

[a]Present address: Joint Institute for Laboratory Astrophysics, University of Colorado and National Bureau of Standards, Boulder, Colo. 80309.

[1]J. Mlynek, N. C. Wong, R. G. deVoe, E. S. Kintzer, and R. G. Brewer, Phys. Rev. Lett. **50**, 993 (1983).

[2]N. C. Wong, E. S. Kintzer, J. Mlynek, R. G. deVoe, and R. G. Brewer, Phys. Rev. B **28**, 4993 (1983).

[3]M. Mitsunaga, E. S. Kintzer, and R. G. Brewer, Phys. Rev. Lett. **52**, 1484 (1984).

[4]J. Manuel and C. Cohen-Tannoudji, C. R. Acad. Sci. **257**, 413 (1963); B. S. Mathur, H. Tang, R. Bulos, and W. Happer, Phys. Rev. Lett. **21**, 1035 (1968).

[5]For a preliminary report, see J. Mlynek, Chr. Tamm, E. Buhr, and N. C. Wong, J. Opt. Soc. Am. **B1**, 492 (1984).

[6]Chr. Tamm, E. Buhr, and J. Mlynek, to be published.

[7]Using saturation spectroscopy, we observed an optical linewidth of $\simeq 5$ MHz (half width at half maximum) for the corresponding Sm transition; this linewidth seemed to be essentially determined by the laser bandwidth.

[8]See, e.g., P. R. Berman, in *Advances in Atomic and Molecular Physics* (Academic, New York, 1977), Vol. 13, p. 57.